MILLIMETER OBSERVATIONS OF CIRCUMSTELLAR DISKS AROUND SUN-LIKE STARS.

V. Roccatagliata, *(roccata@mpia.de)*, Th. Henning, S. Wolf, *Max Planck Institut für Astronomie (MPIA), Königstuhl 17, Heidelberg*, J.M. Carpenter, *California Institute of Technology, Department of Astronomy, Pasadena*, J. Rodmann, *ESA*.

We present the results of a sensitive 1.2 mm continuum survey of a sample of 3 primordial and 33 debris disks around solar-type stars carried out to determine the evolution of debris dust mass as a function of time.

These systems were detected with the Spitzer Space Telescope during an infrared spectrophotometric survey of solar-type stars spanning ages from 3 Myr to 3 Gyr (The Formation and Evolution of Planetary Systems, *FEPS*, Spitzer Space Telescope legacy program - P.I. M. Meyer). Sources older than $\sim$100 Myr are debris disk systems, while the younger systems may represent either the remnants of primordial accretion disks and/or the early stages of the formation of a debris disk. The infrared excess in the spectral energy distribution detected with Spitzer indicates the presence of circumstellar dust. Models of this excess provide an estimation of the dust mass and outer radius of the disk with an uncertainty of orders of magnitude. Our IRAM observations are crucial to constrain disk models measuring, or placing stringent limits, on the mass of dust contained in small grains. Since the millimeter emission from the disk is optically thin, we can derive the disk dust masses from the observed millimeter fluxes, S_ν:

$$M_{\rm dust} = \frac{S_\nu D^2}{k_\nu B_\nu(T_{\rm dust})} \quad (1)$$

where $k_\nu = k_0(\nu/\nu_0)^\beta$ is the mass absorption coefficient, β parameterizes the frequency dependence of k_ν, S_ν is the observed flux, D is the distance to the source, $T_{\rm dust}$ is the dust temperature, $B_\nu(T_{\rm dust})$ is the Planck function. We assumed $k_0 = 1\ {\rm cm}^2/{\rm g}$ at 1.2mm, $\beta = 1$ and $T_{\rm dust}$=40 K.

We have detected 5 sources: ScoPMS52 and $[PZ99]$ J161411.0-230536 (primordial disks), HD 8907, HD 104860 and HD 377 (debris disks). The 1.2 mm fluxes measured and the masses derived from Eq.1 are compiled in Table 1.

For the sample sources with millimeter fluxes not detected at the 3σ level, we compute a dust mass upper limits. In Fig. 1 we present the derived dust masses and the upper limits as a function of their age. We represent as well the results from Carpenter et al. (2005), in order to compare the two studies. Due to the higher sensitivity of the IRAM bolometer compared to SEST (Swedish-ESO Submillimeter Telescope) and OVRO (Owens Valley Radio Observatory), we could detect disks with dust masses of about one order of magnitude less compared to our previous attempt (Carpenter et al. 2005).

We find that there is a steady decline of the disk mass as the system ages which suggests a significant evolution of the disk material. This can be interpreted as a decrease in the mass of the small dust grain particles detectable by our survey and/or changes in the dust opacities. This observational result is also predicted by theretical models. Dominik & Decin (2003) analyze the decrease of the amount of dust with time as a function of the physical mechanism responsible for dust removal. In dense systems (M>$10^{-8} M_\odot$) collisions are the main drivers of dust removal, while in less dense environments the dominant process is the Poynting-Robertson drag. In both cases theoretical models predict a continuous variation of the dust mass with time with a power-law dependence. In the collisional regime the dust mass decrease with t^{-1} while a power-law $M_{\rm dust} \propto t^{-2}$ is characteristic for the Poynting-Robertson regime (Fig.1). Our observations support the first hypothesis, i.e. that collisions are the main mechanism for dust removal in debris disks.

Table 1: 1.2 mm fluxes and the dust masses derived from Eq.1.

Source	Flux (mJy)	Mass ($M_\odot$)
ScoPMS52	5.9 ± 1.4	$5.45 \cdot 10^{-6}$
$[PZ99]$ J161411.0-230536	3.5 ± 1.2	$3.89 \cdot 10^{-6}$
HD 8907	3.2 ± 1.0	$2.15 \cdot 10^{-7}$
HD 104860	4.4 ± 1.2	$5.73 \cdot 10^{-7}$
HD 377	4.0 ± 1.1	$3.59 \cdot 10^{-7}$

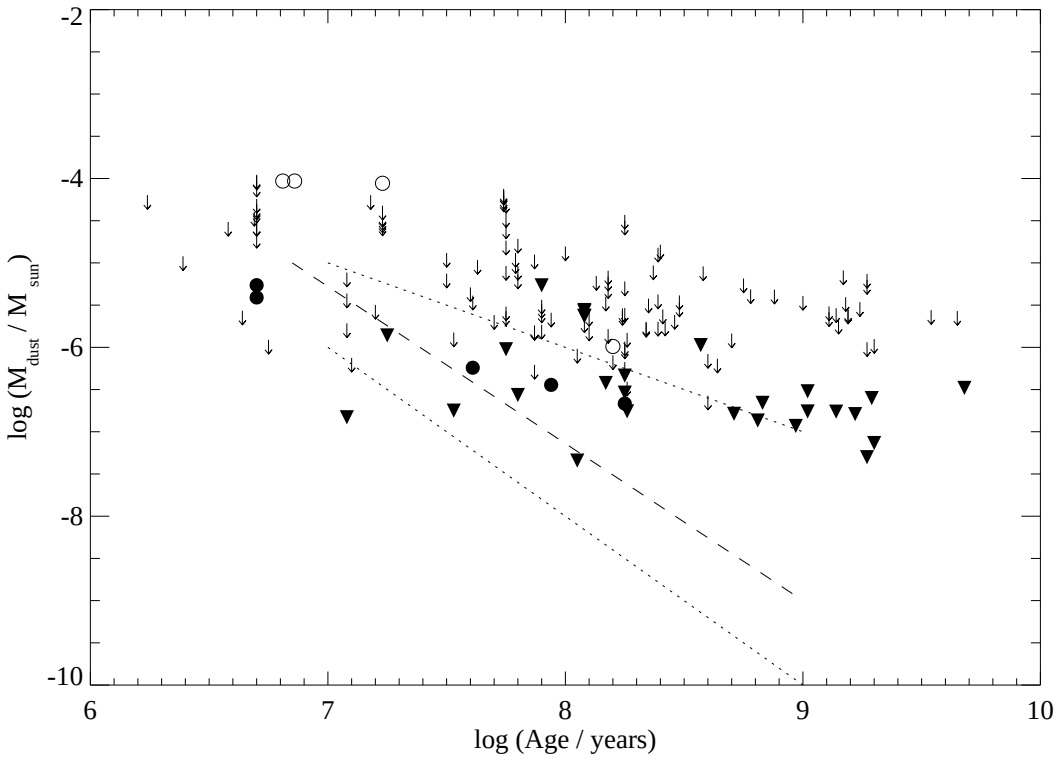

Figure 1: The filled circles represent the masses from our new IRAM detections, while the filled triangles represent the 3σ upper limits. The detections and upper limits from Carpenter et al. (2005) are also shown. The "down" arrows represent the dust mass from the 3σ upper limits, while the empty circles represent the detected masses. The dashed line shows the mass-age relation derived by Spangler et al. (2001) from ISO observations, $M_{\rm dust} \propto$t$^{-1.76}$. The two dotted lines represent the mass-age relations predicted by Dominik&Decin (2003), $M_{\rm dust} \propto t^{-2}$ in Poynting-Robertson regime and $M_{\rm dust} \propto t^{-1}$ in collisional regime.